Table 1. Acid capacity of 1:1 sphingomyelin-sulfatide or 1:1 egg lecithin–sulfatide complexes in several mixtures after correction for the contribution of the excess component.

Composition of systems (μmole)				Acid capacity (μeq H^+/μmole complex)	
Sodium sulfatide	Sphingomyelin	Egg lecithin	Cholesterol	*p*H 7.0–4.0	*p*H 7.0–3.5
7.9	3.2			0.25	0.32
7.6	4.4			.28	.50
7.9	9.5			.30	.45
7.4	8.9			.34	.46
4.4	7.8			.28	.39
8.5	8.5		4.2	.21	.37
8.5	8.8		8.5	.17	.24
8.9		9.3		.20	.31
Comparison with single lipids				*(μeq H^+/μmole lipid)*	
Sphingomyelin				0.083	0.14
Egg lecithin				.044	.058
Sodium sulfatide				.085	.16
Phosphatidylinositol				.28	.37

This frees the phosphate of the choline lipid, which then may be titrated in a manner similar to that for a lipid with an ionizable phosphate, like phosphatidylinositol. This reaction takes place only when the lipids are present in the same particle, as shown when a dispersion of sphingomyelin was mixed with one of sodium sulfatide. Titration showed no interaction of the lipids after 24 hours at 25° or 40°C.

Sphingomyelin-sulfatide systems were prepared with varying mole ratios of these lipids. The acid capacity between *p*H 7 and 3.5 was determined. Again, assuming a complex is formed with a 1 : 1 mole ratio, the capacity of the excess component was deducted from the total which was then divided by the number of moles of complex. These results may be compared with the individual components and with the sodium salt of phosphatidylinositol. The acid capacity of lecithin-sulfatide mixtures was slightly less than that of the sphingomyelin-sulfatide, possibly because the larger area occupied by egg lecithin (*10*) increases the distances between ionic groups.

The incorporation of cholesterol or cerebroside into sphingomyelin or lecithin systems did not change the titration characteristics of these lipids. Cholesterol, however, reduces the titration capacity of sphingomyelin-sulfatide mixtures. As the mole ratio of cholesterol is increased, the acid capacity of the complex decreases (Table 1), an indication that cholesterol molecules may be interposed between the sphingomyelin and sulfatide, increasing the distance between the charged groups.

The choline phospholipids, lecithin and sphingomyelin, are important constituents in many biological membranes. Within such systems, ionic binding between the choline phospholipids and anionic lipids probably occurs, thus adding to the stability of these membranes.

MORRIS B. ABRAMSON
ROBERT KATZMAN

Saul R. Korey Department of
Neurology, Albert Einstein College
of Medicine, Bronx, New York 10461

References and Notes

1. See for example H. Davson and J. F. Danielli, *The Permeability of Natural Membranes* (Cambridge Univ. Press, Cambridge, England, 1952), p. 66; F. A. Vandenheuvel, *J. Amer. Oil Chem. Soc.* **40**, 455 (1963); D. E. Green and A. Tzagoloff, *J. Lipid Res.* **7**, 587 (1966); L. L. M. van Deenen, *Ann. N.Y. Acad. Sci.* **137**, 717 (1966).
2. J. Lenard and S. J. Singer, *Science* **159**, 738 (1968).
3. B. A. Pethica, *Soc. Chem. Ind. London Monograph* **19**, 85 (1965).
4. D. O. Shah and J. H. Schulman [*J. Lipid Res.* **8**, 227 (1967)] present evidence of an internal salt linkage in lecithin monolayers; however, M. Sundaralingam [*Nature* **217**, 35 (1968)] postulates for choline compounds a bond between the nitrogen and the ester oxygen of the phosphate.
5. D. B. Gammack, J. H. Perrin, L. Saunders, *Biochim. Biophys. Acta* **84**, 576 (1964).
6. M. B. Abramson, R. Katzman, H. P. Gregor, *J. Biol. Chem.* **239**, 70 (1964); M. B. Abramson, R. Katzman, C. E. Wilson, H. P. Gregor, *ibid.*, p. 4066; M. B. Abramson, G. Colacicco, R. Curci, M. M. Rapport, *ibid.*, in press; M. B. Abramson, R. Katzman, R. Curci, C. E. Wilson, *Biochemistry* **6**, 295 (1967).
7. M. B. Abramson, W. T. Norton, R. Katzman, *J. Biol. Chem.* **240**, 2389 (1965).
8. M. Lees, J. Folch, G. H. Sloane-Stanley, S. Carr, *J. Neurochem.* **4**, 9 (1959).
9. Egg lecithin was obtained from Sylvana Chemical Co., cholesterol from Eastman Kodak. An MSE ultrasonic generator was used.
10. D. O. Shah and J. H. Schulman, *Biochim. Biophys. Acta* **135**, 184 (1967); *J. Lipid Res.* **6**, 341 (1965).

11. We thank Dr. W. T. Norton for the beef brain sphingomyelin and cerebroside and Dr. M. M. Rapport for a sample of beef heart sphingomyelin as well as for helpful discussion of this work. Supported by Multiple Sclerosis Society grant 503A, U.S. Department of the Interior, Office of Saline Water grant 14-01-0001-1277, and PHS grants NB 03356 and NB 01450.

18 March 1968; revised 17 May 1968

Pyrrhotites: Synthetics Having Two New Superstructures

Abstract. *Synthetic pyrrhotites $Fe_{1-x}S$, synthesized at various compositions and temperatures, show the presence of two new superstructures based on the hexagonal subcell of the NiAs type (axes* A *and* C*): one, in the range* $1-x=0.89$ *to 0.93, has* $a = 90A$ *and* $c = 3C$*; the other, in the range* $1 - x = 0.935$ *to 0.975, has* $a = 2A$ *but* c *irrationally related to* C*, varying with composition.*

Because of its common occurrence and unusual magnetic properties, pyrrhotite $Fe_{1-x}S$ has been extensively studied, but many important questions regarding its phase relations and crystallography remain unanswered. Three different types of pyrrhotite have been confirmed as low-temperature stable phases (*1, 2*), all of which are superstructures of the NiAs type of structure, whose cell dimensions are *A*, about 3.45 Å; *C*, about 5.8 Å. They are

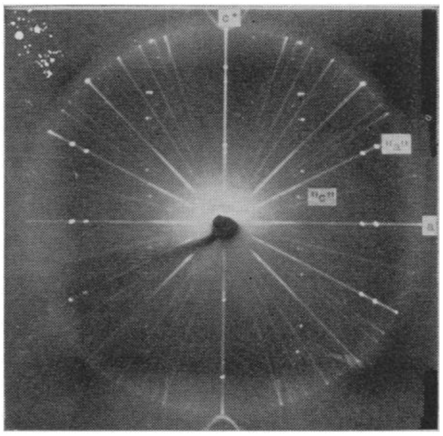

Fig. 1. Precession photograph (010)o* of 3*C*-type pyrrhotite ($Fe_{0.90}S$) quenched from 300°C; Fe*K*α, μ=25 deg, 190 hours. The *a** and *c** axes have been indicated as well as the "*a*"-type and "*c*"-type reflections.

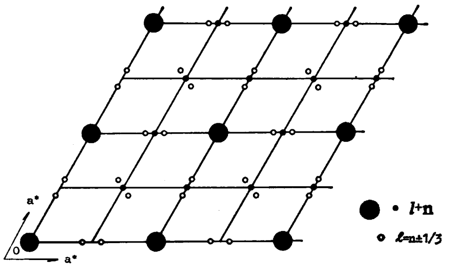

Fig. 2. Reciprocal lattice projected on (001)* of the 3*C* type of pyrrhotite (not to scale). Large solid circles, "*a*"-type reflections; small solid circles, "*b*"-type reflections; open circles, "*c*"-type reflections (see text).

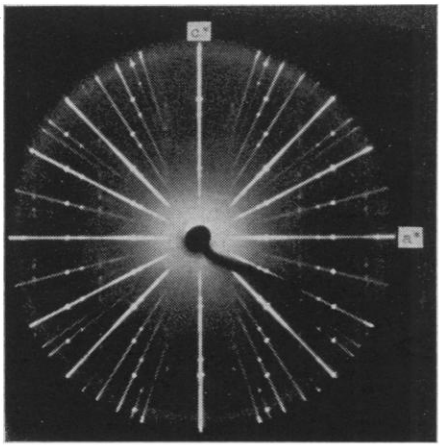

Fig. 3. Precession photograph $(010)_0{}^*$ of nonintegral-type pyrrhotite ($Fe_{0.96}S$) quenched from 250°C; Mo*Kα*, $\mu = 20$ deg, 69 hours. The a^* and c^* axes are indicated.

hexagonal 2*C*-type (triolite, FeS), hexagonal 5*C*-type (FeS–Fe_7S_8), and monoclinic 4*C*-type (Fe_7S_8). A hexagonal 7*C*-type was also described (*2*) as a high-temperature phase extending from FeS to $Fe_{0.835}S$, although the NiAs type of structure has been commonly reported as a high-temperature phase (*3*).

We now report study of synthetic single crystals of pyrrhotite having different chemical compositions; we used x-ray methods (powder, oscillation, and precession) at room temperature and high temperatures (100° to 350°C) with Co*Kα*, Fe*Kα*, and Mo*Kα* radiations.

Our specimens were synthesized from mixtures of sulfur (99.999 percent) and iron (99.99 percent) ranging from FeS to $Fe_{0.89}S$. The mixtures were enclosed in evacuated silica tubes, kept for 48 hours at 600°C, and quenched. After being ground in acetone the products were resealed in new evacuated silica tubes and kept at 600°C for 1 month. The tubes were then annealed at 300° or 250°C for 1 month and quenched to room temperature. The products consisted of small (0.01 to 0.1 mm) single crystals.

Two new hexagonal types of pyrrhotite were found, both being superstructures of the NiAs type of structure. We propose to call them "3*C* type" and "nonintegral type" on the basis of comparison of their *c*-lengths with that of the NiAs type of subcell.

First we shall describe the 3*C* type. The typical precession photograph $(010)_0{}^*$ with the *h0l* reflections (Fig. 1) was taken from a crystal of composition $Fe_{0.90}S$ quenched from 300°C. The reciprocal lattice projected on $(001)^*$ is schematically illustrated (Fig. 2). The observed reflections divide into these three groups on the basis of the reciprocal-space coordinates defining the positions of the reflections:

"*a*"-type reflections: $h,\ k,\ l$

"*b*"-type reflections: $h + \frac{1}{2},\ k,\ l;$

$$h,\ k + \frac{1}{2},\ l$$

"*c*"-type reflections: $(h + \frac{1}{2}) \pm \frac{1}{90},\ k;$

$$h,\ (k + \frac{1}{2}) \pm \frac{1}{90};\ (h + \frac{1}{2}) \pm \frac{1}{90},$$

$$(k + \frac{1}{2}) \mp \frac{1}{90},\ \text{all with}$$

$$l + \frac{1}{3}\ \text{and}\ l - \frac{1}{3}$$

where *h*, *k*, and *l* refer to the NiAs type of subcell. The subcell measures $A = 3.43 \pm 0.01$ Å and $C = 5.70 \pm 0.01$ Å for the specimen of composition $Fe_{0.90}S$. The "*b*"- and "*c*"-type reflections are much weaker than the "*a*" type, but all are sharp. The "*a*"-type reflections correspond to the NiAs type of subcell, and the "*b*"- and "*c*"-type reflections are superstructure reflections. The "*c*"-type reflections occur in pairs close to

$$(h + \frac{1}{2},\ k,\ l \pm \frac{1}{3})$$

$$(h,\ k + \frac{1}{2},\ l \pm \frac{1}{3})$$

$$(h + \frac{1}{2},\ k\frac{1}{2},\ l \pm \frac{1}{3})$$

from which the members of a pair are displaced equal distances in opposite senses along an a^* direction (see Fig. 2).

The intensities of the two reflections forming a pair differ from each other. The interval between paired "*c*"-type reflections is 1/45 of the repeat of the "*a*"-type reflections along the a^* direction. The cell dimensions are $a = 90A$ and $c = 3C$; $Z = 48{,}600(Fe_{1-x}S)$. The space group is $P6_222$ or $P6_422$, for which *l* must be a number 3*n* for a reflection 00*l* to occur. The calculated density, for chemical formula $Fe_{0.90}S$, is 4.75 g/cm^3. This type is called 3*C* because its *c*-length is three times that of the NiAs type of subcell.

Possibly, however, the complex patterns of the hexagonal superstructure are produced by three orthorhombic crystals, having $a = A$, $b = 45\sqrt{3A}$, and $c = 3C$, twinned around a common *c*-axis. For examination of the possibility of a domain structure, crystals of the 3*C* type were cooled slowly (16°C/hour) from 350° to 250°C in a magnetic field of 15,000 gauss. No change in the x-ray patterns was observed.

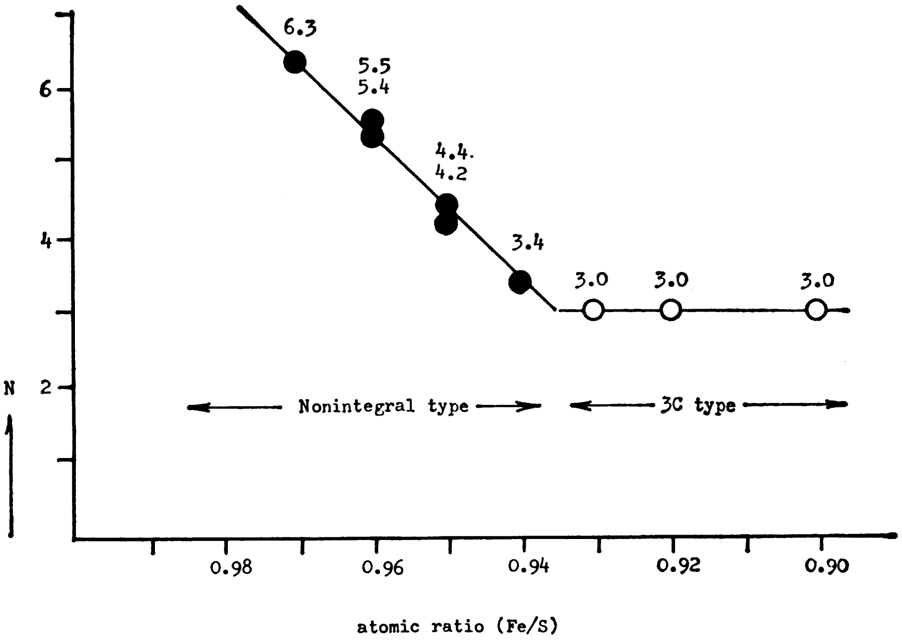

Fig. 4. Relations between chemical composition and *N* ($N = 1/\delta l$; see text) for pyrrhotites of the nonintegral type quenched from 250°C.

This 3*C* type was obtained for specimens between $Fe_{0.91}S$ and $Fe_{0.89}S$ quenched from 300°C, and between $Fe_{0.93}S$ and $Fe_{0.90}S$ quenched from 250°C. Crystals of this type ($Fe_{0.90}S$) were examined at high temperatures with the Nonius-Weissenberg camera; oscillation photographs taken at 290°C around the *c*-axis, after heating at the same temperature for 2 hours, gave the 3*C*-type patterns described. The superstructure reflections, however, disappeared at 320°C, leaving only "*a*"-type reflections. The superstructure reflections reappeared at 290°C and at room temperature soon after the heating; thus the 3*C* type is not a metastable quenched product, but a phase with a range of stability from below the transition temperature to the high-temperature phase at about 310°C. This finding confirms the transition (*4*) at about 315°C of pyrrhotite $\sim Fe_{0.90}S$ to the high-temperature NiAs type, and indicates that the 7*C* type (*2*) is a phase produced by quenching.

Now we describe the nonintegral type. The typical precession photograph $(010)_0^*$ with the *h*0*l* reflections (Fig. 3) was taken from a crystal, of composition $Fe_{0.96}S$, quenched from 250°C. Only two groups of reflections are observed: the "*a*"-type reflections have the same indices here as in the 3*C* type; the "*b*"-type reflections are not observed; the "*c*"-type reflections, observed in pairs along the a^* direction in the 3*C* type, are here isolated and diffuse along the c^* direction. The reciprocal-space coordinates defining the positions of the intensity maxima of the "*c*"-type reflections were obtained from the specimens quenched from 250°C, because the "*c*"-type reflections are extremely diffuse for the specimens quenched from 300°C; they are

$$(h + \frac{1}{2}, k, l \pm \delta l)$$

$$(h, k + \frac{1}{2}, l \pm \delta l)$$

$$(h + \frac{1}{2}, k + \frac{1}{2}, l \pm \delta l)$$

where δl is positive and nonintegral. The value of δl varies continuously from $\frac{1}{3}$ to $\frac{1}{7}$ with chemical composition. Because the specimens of this type are conventionaly expressed by the values of the apparent *c*-length (*NC*, where $N = 1/\delta l$ is generally nonintegral), this type is called nonintegral. The relation between the value of *N* and chemical composition is illustrated for specimens quenched from 250°C (Fig. 4). The nonintegral type for the special case $N = 3$ differs from the 3*C* type, although both crystals have the same $c = 3C$. The "*c*"-type reflections are sharp and appear in pairs giving $a = 90A$ in the 3*C* crystals, while they appear as single reflections with diffuseness along c^* and give $a = 2A$ in the nonintegral type of crystals.

The nonintegral type was observed for specimens between $Fe_{0.97}S$ and $Fe_{0.92}S$ quenched from 300°C, and between $Fe_{0.97}S$ and $Fe_{0.94}S$ quenched from 250°C (Fig. 4). For investigation of their stability range, crystals of the nonintegral type were examined at high temperatures by the precession method. The "*c*"-type reflections from crystals $Fe_{0.95}S$ were very diffuse at 100°C and completely disappeared at 150°C, while those from crystals $Fe_{0.94}S$ completely disappeared at 200°C. Thus the transition temperature of the nonintegral type to the NiAs type depends on chemical composition.

The conspicuous variations, of the intensity maxima of the "*c*"-type reflections with composition, in pyrrhotites of the nonintegral type are quite similar to those of the "*e*"- and "*f*"-type reflections observed in plagioclase feldspars (*5*). Pyrrhotite is the first example of sulfides, as far as we know, in which superstructure reflections of the nonintegral type are confirmed; such reflections were also observed in the Cu-S system (*6*) and seem to be common in synthetic sulfides with solid-solution ranges. All natural pyrrhotites so far described have superstructures of the 2*C*, 4*C*, and 5*C* types, in which the cells are multiples of the NiAs type of subcell. These superstructures can be called integral types in contradistinction from the nonintegral type. Pyrrhotites of the nonintegral type are stable below the transition to the high-temperature form, but are considered to change to the low-temperature forms with superstructures of integral types.

NOBUO MORIMOTO
HIROMOTO NAKAZAWA
Institute of Scientific and Industrial Research, Osaka University, Yamada Kami, Suita, Osaka, Japan

References and Notes

1. R. H. Carpenter and G. A. Desborough, *Amer. Mineralogist* **49**, 1350 (1964).
2. G. A. Desborough and R. H. Carpenter, *Econ. Geol.* **60**, 1431 (1965).
3. F. Grønvold and H. Haraldsen, *Acta Chem. Scand.* **6**, 1452 (1952).
4. H. S. Roberts, *J. Amer. Chem. Soc.* **57**, 1034 (1935).
5. M. G. Bown and P. Gay, *Z. Krist.* **111**, 1 (1958); H. D. Megaw, *Proc. Roy. Soc. London Ser. A.* **259**, 59, 159, 184 (1960).
6. N. Morimoto and K. Koto, in preparation.
7. We thank J. D. H. Donnay for reviewing and improving the manuscript.

2 April 1968

■

Bends: Detection of Circulating Gas Emboli with External Sensor

Abstract. Circulating gas emboli associated with rapid decompression are detectable in superficial vessels of animals by the use of an ultrasonic Doppler flowmeter transducer which is applied externally.

Gas embolism of capillary beds resulting from rapid decompression is believed to be largely responsible for the symptom complex commonly referred to as "the bends" (*1*). We demonstrated (*2*) that a surgically implanted Doppler ultrasonic blood flowmeter (*3*) can detect circulating gas emboli in the caudal vena cava of swine well before the first decompression stop recommended for man (*4*). We now describe an atraumatic, nonsurgical method for transcutaneous detection of circulating gas emboli in superficial vessels; our experience with three animal species suggests that the technique may have direct application to the prevention and treatment of the bends in human divers.

The Doppler flowmeter (*3*) measures velocity of blood flow by detecting the frequency shift incurred by ultrasound that is scattered from moving blood cells which produce audio signals whose amplitude depends on the scattering efficiency of the cells. Since gas bubbles are highly efficient scatterers, a gas embolus passing through the ultrasonic field produces a marked transient increase in the audio signal amplitude, with a characteristic sound best described as a "chirp." These artifacts are easily heard and may be discriminated electronically (*2*). Although the flowmeter was originally designed for chron-